RSC Advances

PAPER

View Article Online
View Journal | View Issue

Cite this: *RSC Adv.*, 2019, **9**, 19495

Effects of Mo alloying on stability and diffusion of hydrogen in the $Nb_{16}H$ phase: a first-principles investigation

Dianhui Wang, †[a] Yang Wu,†[a] Zhenzhen Wan,[a] Feng Wang,[a] Zhongmin Wang,*[ab] Chaohao Hu, *[ab] Xiaotian Wang *[c] and Huaiying Zhou[ab]

Received 6th May 2019
Accepted 14th June 2019

DOI: 10.1039/c9ra03401c

rsc.li/rsc-advances

First-principles calculations and the method of climbing-image nudged elastic band were used to investigate the effects of Mo alloying on the structural stability, mechanical properties, and hydrogen-diffusion behavior in the $Nb_{16}H$ phase. The $Nb_{12}Mo_4H$ phase (26.5 at% Mo) was found to be the most thermodynamically stable structure, with a low ΔH_f value (−0.26 eV) and high elastic modulus. Calculations revealed that the tetrahedral interstitial site (TIS) was the predominant location of H in both $Nb_{16}H$ and $Nb_{12}Mo_4H$ phases. The calculated H-diffusion energy barrier and the diffusion coefficient of the $Nb_{12}Mo_4H$ phase were 0.153 eV and 5.65×10^{-6} cm^2 s^{-1} (300 K), respectively, which suggest that the addition of Mo would lead to a lower energy barrier and high diffusion coefficients for the $Nb_{16}H$ phase, thus improving the hydrogen-permeation properties of Nb metal.

1. Introduction

Hydrogen is not only an important raw material for chemical and petrochemical industries, but also a potential clean fuel as well as a good energy carrier. Pure hydrogen does not exist as a natural resource like coal and oil, however. Since it has to be produced from hydrogen-containing compounds, a safe, low-cost, and highly efficient separation and purification technology is always required. Hydrogen-permeable alloy membranes have been well regarded as the most important materials for hydrogen separation and purification.[1–5] Currently, group V metals (vanadium, niobium, and tantalum) have attracted many investigations as promising hydrogen-separation materials owing to their lower price and higher hydrogen permeability than those of currently used Pd-based alloys.[3,6] However, there is still a large barrier to practical application of these metals because of their poor resistance to hydrogen embrittlement.[3,7,8] Experimental studies have verified that alloying the metals is an effective way to solve this problem.[6–9]

Niobium is one of the most promising hydrogen-permeable candidates for membranes because it possesses a good combination of excellent high-temperature mechanical properties and corrosion resistance.[10–12] Recent theoretical research performed by Watanabe *et al.* revealed that the addition of W could decrease the hydrogen solubility in Nb and therefore improve its resistance to hydrogen embrittlement.[6,13] Hu *et al.* performed a similar study and found that the addition of W can improve the mechanical properties of the $Nb_{16}H$ phase, decrease the structural stability of the $Nb_{15}WH$ (tetrahedral (T)) phase, lower the diffusion barrier of H, and enhance diffusion paths for H.[14] Both W and Mo are high-*Z* refractory metals (*i.e.*, refractory metals containing impurities with high atomic numbers (*Z*)) with similar physical properties. Moreover, Mo has several characteristic properties: compared with W, Mo has a lower melting point (2883 K) and a lower erosion rate, while H has higher diffusivity and lower solubility in Mo, leading to lower H retention.[15–17] These characteristics make Mo an important alloying candidate for Nb-based alloy membranes for hydrogen permeation. However, since relevant works have not been reported in the literature, it is necessary to engage in first-principles theoretical investigations that are free from any experimental limitations on the effect of Mo addition on the structure and diffusion properties of the NbH phase in a first-principles way. Such calculations will also contribute to the understanding and design of H-storage and H-separation materials based on Nb.

The effects of the addition of Mo to the electronic structure, structural stability, H diffusion, and mechanical properties of the NbH phase were investigated by first-principles calculation based on density functional theory. $Nb_{16}H$ was purposely selected and four Mo atoms were added to reach the equivalent of an experimental composition of 25 at% Mo in NbH.[6,7,13,18] The

[a]*School of Materials Science and Engineering, Guilin University of Electronic Technology, Guilin 541004, P. R. China. E-mail: zmwang@guet.edu.cn; chaohao.hu@guet.edu.cn*

[b]*Guangxi Key Laboratory of Information Materials, Guilin University of Electronic Technology, Guilin 541004, P. R. China*

[c]*School of Physical Science and Technology, Southwest University, Chongqing 400715, P. R. China. E-mail: xiaotianwang@swu.edu.cn*

† These authors contributed equally to this work.

calculated results revealed that such addition would lead to a lower energy barrier of H diffusion, a higher diffusion coefficient, and improved mechanical properties.

2. Computational method

The calculations were carried out by using the Vienna Ab-initio Simulation Package (VASP).[19] The interactions between core and valence electrons were described with the projector augmented wave (PAW).[20] The exchange and correlation functions were generalized gradient approximations (GGAs) developed by Perdew *et al.*[21] An energy cutoff of 360 eV was used for the plane-wave basis sets, and the K points set used in our calculations is $5 \times 5 \times 5$ grid generated by Monkhorst–Pack schema.[22] During structure relaxation of the lattice parameters, the volume and atomic positions were fully optimized with in-symmetry restrictions until the total energy converged to 10^{-5} eV in the self-consistent loop, and the criterion of force used in the calculations is 0.01 eV Å^{-1} atom^{-1}.

Accordingly, we built supercell models of basic defect structures in which a H atom was placed at the tetrahedral interstitial site (TIS) and another at the octahedral interstitial site (OIS). A unit cell of $2 \times 2 \times 2$ (16 atoms) with a body-centered cubic (BCC) structure[23] was selected for pure Nb, and a Mo atom was introduced to replace the Nb atom—a series of structures with the composition $Nb_{16-x}Mo_x$ was thus obtained. One H atom was then added at the TIS and one at the OIS of BCC Nb and $Nb_{16-x}Mo_x$. Fig. 1 shows the schematic illustrations of $Nb_{16-x}Mo_xH$ ($x = 4$) with TIS and OIS.

To probe the diffusion properties of hydrogen in the bulk of the Nb–Mo alloy, the climbing image nudged elastic band (CI-NEB) method[24] was used to determine the diffusion barriers between the initial and final positions. Four images were taken and all the images were relaxed until the maximum force on each atom was less than 0.01 eV Å^{-1} and the other computational parameters were the same as the above.

The diffusion coefficient (D) is also an important index that determines the diffusion velocity of H. According to the Arrhenius diffusion equation, D can be expressed by $D = D_0 \exp(-E_a/kT)$, where the D_0, E_a, k, and T are the pre-exponential factor, diffusion energy barrier, the Boltzmann constant, and the absolute temperature, respectively. For a metal with a cubic structure, D_0 can be expressed as $D_0 = \frac{1}{6}r^2\nu$, where r and ν are the jump distance and the vibration frequency, respectively. We calculated ν according to Zener and Wert's theory,[25] which is approximately expressed by $\nu = \sqrt{2E_a/mr^2}$, where m is the mass of the impurity atom. As it is already known that the mass of the H atom is 1.67×10^{-27} kg, the jumping distance of the TIS H in Nb was set as $a/2\sqrt{2}$ Å.

3. Results and discussion

3.1. Structure stability of $Nb_{16-x}Mo_xH$ phases

In order to investigate the effect of the amount of alloying Mo on the stability of the $Nb_{16}H$ phase, the heats of formation (ΔH_f) of various $Nb_{16-x}Mo_xH$ ($x = 0$, 1, 2, 3, 4, 5, and 6) phases were calculated from the following equations:

$$\Delta H_f(Nb_{16}H) = E_{Nb_{16}H} - 16E_{Nb} - \frac{1}{2}E_{H_2}, \quad (1)$$

$$\Delta H_f(Nb_{16-x}Mo_xH) = E_{Nb_{16-x}Mo_xH} - E_{Nb_{16-x}Mo_x} - \frac{1}{2}E_{H_2}, \quad (2)$$

where $E_{Nb_{16}H}$, $E_{Nb_{16-x}Mo_xH}$, $E_{Nb_{16-x}Mo_x}$, E_{Nb} and E_{H_2} are the total energies of $Nb_{16}H$, $Nb_{16-x}Mo_xH$, $Nb_{16-x}Mo_x$, BCC Nb (ground state), and a H_2 molecule, respectively. The obtained ΔH_f values of the $Nb_{16-x}Mo_xH$ phases are presented in Fig. 2 and Table 1.

Several characteristics can be derived from Fig. 2 and Table 1. First, all of the $Nb_{16-x}Mo_xH$ phases are energetically favorable, with negative ΔH_f values. The absolute values of ΔH_f are very small (less than 0.2 eV), indicating that the $Nb_{16-x}Mo_xH$ phases can be stable. Second, the absolute value of the formation enthalpy of $Nb_{16-x}Mo_xH$ increases as the amount of alloying Mo increases from $x = 0$ to $x = 4$; it then decreases when x is above 4. The $Nb_{12}Mo_4H$ phase has the highest

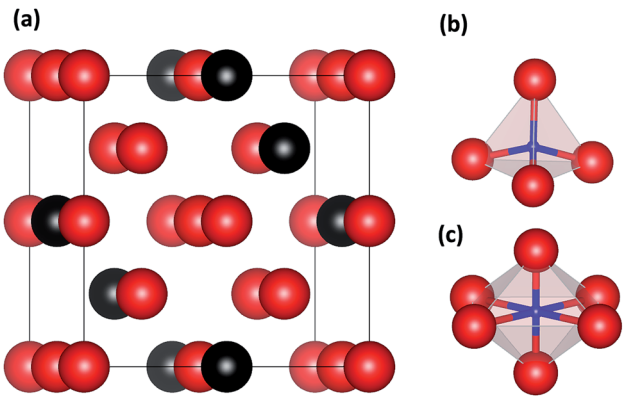

Fig. 1 Crystal models of (a) $Nb_{12}Mo_4H$, (b) a tetrahedral interstitial site (TIS), and (c) an octahedral interstitial site (OIS). The red and black balls represent Nb and Mo atoms, respectively. The small blue balls represent various sites of H atoms.

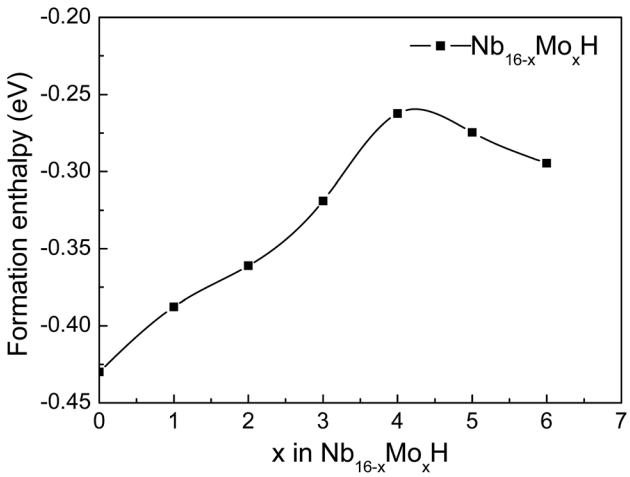

Fig. 2 Formation enthalpies of $Nb_{16-x}Mo_xH$ ($x = 0$, 1, 2, 3, 4, 5, 6) phases.

Table 1 Calculated lattice constants (a), elastic constants (C_{ij}), bulk modulus (B), shear modulus (G), and Young's modulus (E) of Nb_{16}, $Nb_{16}H$, and $Nb_{12}Mo_4H$ phases

Phase	Lattice constant, a (Å)	Mechanical property (GPa)											
		C_{11}	C_{12}	C_{13}	C_{23}	C_{22}	C_{33}	C_{44}	C_{55}	C_{66}	B	G	E
Nb_{16}	6.60	244	139.3					13.7			174.2	24.3	69.7
$Nb_{16}H$ (TIS)	6.63	245	137.8	138			247.2	25.4		26.5	173.8	34.8	98
$Nb_{16}H$ (OIS)	6.58	242	148.3	128			274.4	14.5		13.7	174.1	26	74.4
$Nb_{12}Mo_4H$ (TIS)	6.53	311	137.4	143	139.2	278.9	317.6	31.6	39	39.7	194.9	50.6	139.7

absolute value of ΔH_f, which is favorable for the dehydrogenation of the $Nb_{16-x}Mo_xH$ phase. Therefore, $Nb_{12}Mo_4H$ was selected for further study. Third, the calculated formation enthalpy absolute values of $Nb_{16}H$ (TIS) and $Nb_{16}H$ (OIS) are 0.43 and 0.09 eV, respectively. $Nb_{16}H$ (TIS) has a clearly higher absolute value of 0.43 eV, which indicates that the TIS is thermodynamically more possible than the OIS for H in BCC Nb. Such results are in excellent agreement with similar experimental observations[26–28] and theoretical work[14] reported in the literature. Since the addition of Mo has no effect on the preferred location of H, and TIS is the predominant location of H in both $Nb_{16}H$ and $Nb_{12}Mo_4H$ phases, only the $Nb_{12}Mo_4H$ (TIS) phase was selected for further investigation of its mechanical properties. In addition, the $Nb_{12}Mo_4H$ (TIS) phase is energetically less favorable, with higher ΔH_f value than the corresponding $Nb_{16}H$ (TIS), suggesting that the addition of Mo would decrease the solubility of H in the TIS of Nb. A possible explanation has been offered by Yukawa *et al.*: the higher ΔH_f basically induces an decrease in H solubility and hydrogen embrittlement.[7,13,18]

After the series of calculations for the supercell models, the lattice constants (a) of various $Nb_{16}H$ and $Nb_{12}Mo_4H$ phases were obtained; the results are listed in Table 1. The calculated lattice constants of pure Nb, $Nb_{16}H$ (TIS and OIS) and $Nb_{12}Mo_4H$ (TIS) are 6.60, 6.63, 6.58, and 6.53 Å, respectively. The values of pure Nb and $Nb_{16}H$ (TIS) match well with the corresponding experimental unit cell values of 6.61 and 6.63 Å.[26–28] In addition, Mo has a smaller atomic radius than Nb, which may lead to a slight decrease in the lattice constant with the addition of Mo to the $Nb_{16}H$ phase.

3.2. Mechanical properties of $Nb_{16}H$ and $Nb_{12}Mo_4H$ phases

To find out the effect of Mo alloying on the mechanical properties of Nb hydride, the elastic constants of $Nb_{16}H$ (TIS and OIS), $Nb_{12}Mo_4H$ (TIS), and pure Nb were calculated for comparison. The specified elastic constant was obtained by analyzing the difference between the total energy of the original cell and that of the deformed cell under a series of small strains. For the BCC crystal of Nb, there are three independent components of elastic constants: C_{11}, C_{12}, and C_{44}. $Nb_{16}H$ has tetragonal symmetry and possesses three more components: C_{13}, C_{33}, and C_{66}. Mo doping reduces the symmetry to orthorhombic and thus adds two components: C_{22} and C_{23}.[29,30] The calculated elastic constants are listed in Table 1.

According to the equations of elastic moduli and the criteria for mechanical stability, the mechanical stability is defined by the following restrictions for a tetragonal crystal:[31,32]

$$\begin{gathered} C_{11} > 0, C_{33} > 0, C_{44} > 0, C_{66} > 0, \\ (C_{11} - C_{12}) > 0, \\ (C_{11} + C_{33} - 2C_{13}) > 0, \\ [2(C_{11} + C_{12}) + C_{33} + 4C_{13}] > 0. \end{gathered} \tag{3}$$

For an orthorhombic crystal, the criteria of mechanical stability are given by

$$\begin{gathered} C_{11} > 0, C_{22} > 0, C_{33} > 0, C_{44} > 0, C_{55} > 0, C_{66} > 0, \\ C_{11} + C_{22} + C_{33} + 2(C_{12} + C_{13} + C_{23}) > 0, \\ C_{11} + C_{22} - 2C_{12} > 0, C_{11} + C_{33} - 2C_{13} > 0, \\ C_{22} + C_{33} - 2C_{23} > 0. \end{gathered} \tag{4}$$

The results of elastic constants, C_{ij}, indicate that both $Nb_{16}H$ and $Nb_{12}Mo_4H$ phases meet the criteria for mechanical stability.

The obtained elastic constants were then used to calculate the bulk modulus (B) and shear modulus (G) from the Voigt–Reuss–Hill approximations.[33,34] The Young's modulus (E) is determined using the equation $E = 9BG/(3B + G)$.[31] The values of B, G, and E of the $Nb_{12}Mo_4H$ (TIS) phase are larger than those of the $Nb_{16}H$ (TIS and OIS) phase, indicating that Mo alloying improves the mechanical properties of the $Nb_{16}H$ phase, which possibly enhances the resistance against hydrogen embrittlement.

3.3. Electronic properties of $Nb_{16}H$ (TIS) and $Nb_{12}Mo_4H$ (TIS)

Fig. 3 displays the projected density of states (PDOS) of H atoms in the $Nb_{16}H$ (TIS) phase and the $Nb_{12}Mo_4H$ (TIS) phase. It can be seen that there is an obvious difference between the PDOS of $Nb_{16}H$ (TIS) and that of $Nb_{12}Mo_4H$ (TIS). The PDOS peaks at about −6.8 eV are primarily Nb d states in $Nb_{16}H$ (TIS), whereas the PDOS peaks of $Nb_{12}Mo_4H$ (TIS) are dominated by the overlapping H s, Nb d, and Mo d states, indicating that the H atoms penetrated the alloy and bonded with the Nb atoms. After doping with Mo atoms, the hybridizations peaks between the H s state and the Nb d state are smaller and shifted toward lower energy. Fig. 4 shows the total density of states (TDOS) of H atoms in the $Nb_{16}H$ (TIS) and $Nb_{12}Mo_4H$ phases. Compared with the TDOS of the $Nb_{16}H$ (TIS) phase, the TDOS of the $Nb_{12}Mo_4H$ (TIS) below the Fermi level (E_F) are shifted leftward

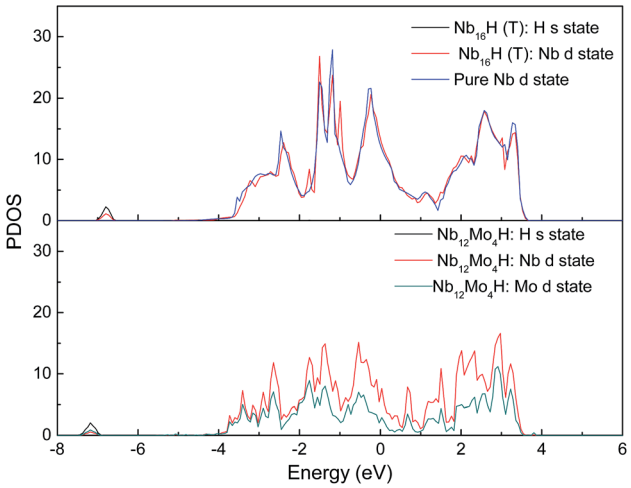

Fig. 3 Comparison of the projected density of states (PDOS) of $Nb_{16}H$ (TIS) and $Nb_{12}Mo_4H$ (TIS) phases.

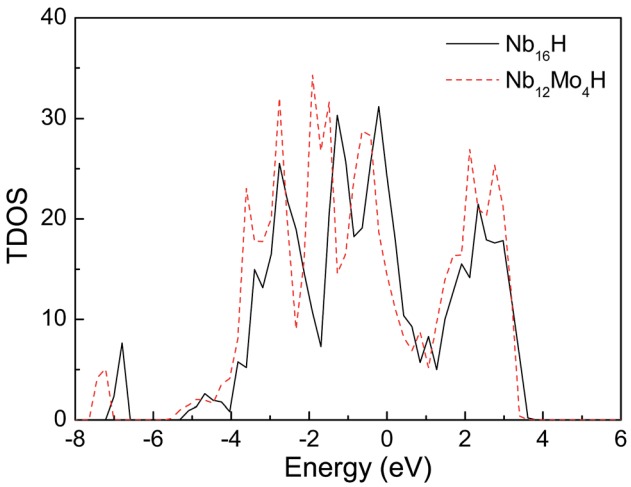

Fig. 4 Comparison of total density of states of $Nb_{16}H$ (TIS) and $Nb_{12}Mo_4H$ (TIS) phases.

to the positions with slightly higher binding energies. These features of electronic structures suggest that the $Nb_{12}Mo_4H$ (TIS) phase should have a stronger chemical bonding than $Nb_{16}H$ (TIS), which is beneficial to hydrogen permeation and should help one understand the improved mechanical properties (B, E, and G) shown in Table 1. In addition, the PDOS peaks are energetically degenerate with the addition of Mo in all regions, which indicate that the Nb–H hybridization is remarkable and favorable for improving the stability of the corresponding system.

3.4. Diffusion and permeation of H in Nb and $Nb_{12}Mo_4$

Next, we investigated the effect of Mo addition on the diffusion of hydrogen in the $Nb_{16}H$ and $Nb_{12}Mo_4H$ phases. The CI-NEB method was used to determine the minimum-energy path and the corresponding energy barrier for the process of H diffusion in the Nb and $Nb_{12}Mo_4$ phases.[35–37] For both Nb and $Nb_{12}Mo_4$, there are three possible paths of H diffusion between TIS and OIS, namely, from TIS to TIS, from TIS to OIS, and from OIS to OIS. Since the diffusion path from OIS to OIS cannot not be realized because the TIS is just located along the path, it was excluded in our study.[38–40]

We first investigated the pathways of H in the bulk of pure Nb. Generally, there are two pathways for H to diffuse in a BCC lattice, *i.e.*, TIS → TIS and TIS → OIS. It can be clearly seen that the energy barrier from TIS to TIS in Nb is 0.225 eV, which is much lower than the corresponding value of 0.362 eV from TIS to OIS, suggesting that the diffusion path of H in bulk Nb should be mainly from TIS to TIS instead of TIS to OIS. For H diffusion in the $Nb_{12}Mo_4$ alloy, it can be clearly seen in Fig. 5 and 6 that the energy barrier from TIS to TIS (0.157 eV) is smaller than the corresponding value in Nb, and a similar observation can be seen from TIS to OIS. The above comparison demonstrates that the addition of Mo in Nb can make H diffusion easier with a smaller energy barrier.

The H-diffusion energy barrier calculated for pure Nb and the $Nb_{12}Mo_4$ alloy is 0.225 and 0.157 eV, respectively. The vibration frequency of pure Nb and the $Nb_{12}Mo_4$ alloy is 2.686×10^{13} s^{-1} and 2.345×10^{13} s^{-1}, respectively. According to the Arrhenius diffusion equation, the calculated diffusion

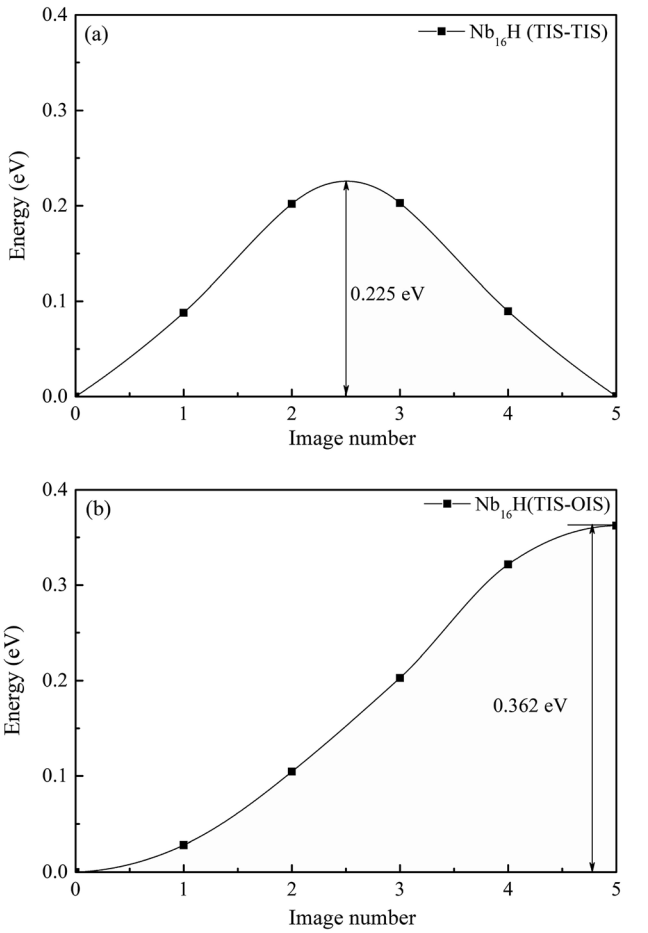

Fig. 5 Migration barrier of H diffusion (a) from TIS to TIS and (b) from TIS to OIS in the $Nb_{16}H$ phase.

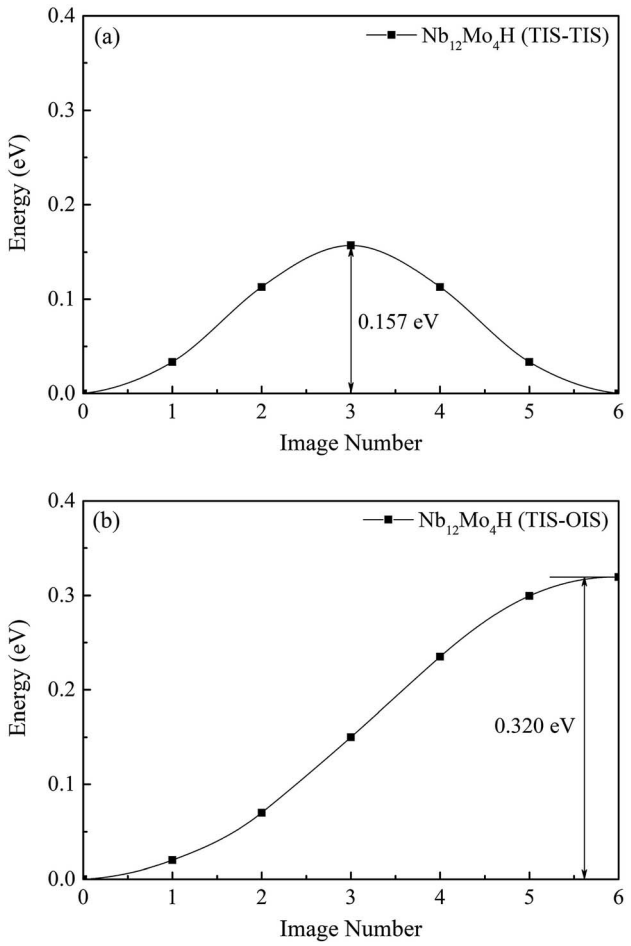

Fig. 6 Migration barrier of H diffusion (a) from TIS to TIS and (b) from TIS to OIS in the $Nb_{12}Mo_4H$ phase.

coefficient is 8.87×10^{-7} cm^2 s^{-1} for pure Nb and 5.65×10^{-6} cm^2 s^{-1} for the $Nb_{12}Mo_4$ phase at the standard room temperature of 300 K. From the above analysis, it can be deduced that the addition of Mo should have an important effect on the diffusion of H in Nb, *i.e.*, H diffusion in the $Nb_{12}Mo_4$ phase should become energetically more favorable when the energy barrier is lower. These characteristics would therefore bring about an increase in the H-diffusion coefficient and an improvement in H permeability. In other words, the addition of Mo could lower the diffusion barrier of H, which would fundamentally lead to higher H diffusion and high H permeability in the $Nb_{12}Mo_4H$ phase.

4. Conclusions

We used first-principles calculations and the CI-NEB method to perform a comprehensive study on the effects of Mo on the structural stability and mechanical properties of the $Nb_{16}H$ phase and the diffusion of hydrogen through the alloy. The calculations revealed that the $Nb_{12}Mo_4H$ phase is the most thermodynamically stable structure with a low ΔH_f of about −0.26 eV and a high elastic modulus. The diffusion paths of H in both Nb and $Nb_{12}Mo_4$ phases should be mainly from TIS to TIS. The calculated H-diffusion energy barrier and the diffusion coefficient are 0.153 eV and 5.65×10^{-6} cm^2 s^{-1} (at 300 K), respectively. The lower energy barrier and higher diffusion coefficient of the $Nb_{12}Mo_4$ phase imply that the addition of a suitable amount of Mo could improve hydrogen permeation in Nb metal.

Conflicts of interest

None.

Acknowledgements

This work was supported by the National Natural Science Foundation of China (51471055, 51401060, and 11464008), the Natural Foundations of Guangxi Province (2016GXNSFGA380001 and 2014GXNSFGA118001), and the Guangxi Key Laboratory of Information Materials (171001-Z) and the Guangxi Postgraduate Innovation Project (YCSW2018144).

References

1 E. Kikuchi, Membrane reactor application to hydrogen production, *Catal. Today*, 2000, **56**, 97–101.
2 Y. Wu, Z. M. Wang, D. H. Wang, Z. Z. Wan, Y. Zhong, C. H. Hu and H. Y. Zhou, Effects of Ni doping on various properties of NbH phases: A first-principles investigation, *Sci. Rep.*, 2017, **7**(1), 6535.
3 S. C. Chen, C. Y. Hung, G. C. Tu and M. H. Rei, Perturbed hydrogen permeation of a hydrogen mixture-new phenomena in hydrogen permeation by Pd membrane, *Int. J. Hydrogen Energy*, 2008, **33**(7), 1880–1889.
4 C. Y. Hao, Y. Wu, Y. J. An, B. H. Cui, J. N. Lin, X. N. Li, D. H. Wang, M. H. Jiang, Z. X. Cheng and S. Hu, Interface-coupling of CoFe-LDH on MXene as high-performance oxygen evolution catalyst, *Materials Today Energy*, 2019, **12**, 453–462.
5 A. Suzuki, H. Yukawa, T. Nambu, Y. Matsumoto and Y. Murata, Analysis of pressure–composition–isotherms for design of non-Pd-based alloy membranes with high hydrogen permeability and strong resistance to hydrogen embrittlement, *J. Membr. Sci.*, 2016, **503**, 110–115.
6 N. Watanabe, H. Yukawa, T. Nambu, Y. Matsumoto, G. X. Zhang and M. Morinaga, Alloying effects of Ru and W on the resistance to hydrogen embrittlement and hydrogen permeability of niobium, *J. Alloys Compd.*, 2009, **477**, 851–854.
7 G. X. Zhang, H. Yukawa, T. Nambu, Y. Matsumoto and M. Morinaga, Alloying effects of Ru and W on hydrogen diffusivity during hydrogen permeation through Nb-based hydrogen permeable membranes, *Int. J. Hydrogen Energy*, 2010, **35**, 1245–1249.
8 J. R. Slining and D. A. Koss, Solid solution strengthening of high purity niobium alloys, *Metall. Trans.*, 1973, **4**, 1261–1264.

9 S. Kozhakhmetov, N. Sidorov, V. Piven, I. Sipatov, I. Gabis and B. Arinov, Alloys based on Group 5 metals for hydrogen purification membranes, *J. Alloys Compd.*, 2015, **645**, S36–S40.

10 Z. H. Liu and J. X. Shang, Elastic properties of Nb-based alloys by using the density functional theory, *Chin. Phys. B*, 2012, **21**, 016202–016206.

11 P. Khowash, S. Gowtham and R. Pandey, Electronic structure calculations of substitutional and interstitial hydrogen in Nb, *Solid State Commun.*, 2012, **152**, 788–790.

12 D. T. Peterson, A. B. Hull and B. A. Loomis, Hydrogen embrittlement considerations in niobium-base alloys for application in the ITER divertor, *J. Nucl. Mater.*, 1992, **191–194**, 430–432.

13 H. Yukawa, T. Nambu, Y. Matsumoto, N. Watanabe, G. X. Zhang and M. Morinaga, Alloy design of Nb-based hydrogen permeable membrane with strong resistance to hydrogen embrittlement, *Mater. Trans. JIM*, 2008, **49**, 2202–2207.

14 Y. T. Hu, H. Gong and L. Chen, Fundamental effects of W alloying on various properties of NbH phases, *Int. J. Hydrogen Energy*, 2015, **40**, 12745–12749.

15 S. Nagata and K. Takahiro, *J. Nucl. Mater.*, 2000, **283–287**, 1038–1042.

16 C. Duan, Y. L. Liu, H. B. Zhou, Y. Zhang, S. Jin, G. H. Lu, *et al.*, First-principles study on dissolution and diffusion properties of hydrogen in molybdenum, *J. Nucl. Mater.*, 2010, **404**, 109–115.

17 G. M. Wright, D. G. Whyte and B. Lipschultz, *J. Nucl. Mater.*, 2009, **390–391**, 544–549.

18 H. Yukawa, G. X. Zhang, N. Watanabe, M. Morinaga, T. Nambu and Y. Matsumoto, Analysis of hydrogen diffusion coefficient during hydrogen permeation through niobium and its alloys, *J. Alloys Compd.*, 2009, **476**, 102–106.

19 G. Kresse and J. Furthmüller, *Phys. Rev. B: Condens. Matter Mater. Phys.*, 1996, **54**, 11169.

20 P. E. Blochl, *Phys. Rev. B: Condens. Matter Mater. Phys.*, 1994, **50**, 17953.

21 J. P. Perdew, J. A. Chevary, S. H. Vosko, K. A. Jackson, M. R. Pederson, D. J. Singh, *et al.*, Atoms, molecules, solids, and surfaces: applications of the generalized gradient approximation for exchange and correlation, *Phys. Rev. B: Condens. Matter Mater. Phys.*, 1992, **46**, 6671–6687.

22 M. Methfessel and A. T. Paxton, High-precision sampling for Brillouin-zone integration in metals, *Phys. Rev. B: Condens. Matter Mater. Phys.*, 1989, **40**, 3616–3621.

23 J. H. Long and H. Gong, Ab initio calculation of NbH phases with low H compositions, *Int. J. Hydrogen Energy*, 2014, **39**, 11798–11806.

24 R. Frauenfelder, Solution and Diffusion of Hydrogen in Tungsten, *J. Vac. Sci. Technol.*, 1969, **6**, 388.

25 G. Henkelman, B. P. Uberuaga and H. Jónsson, *J. Chem. Phys.*, 2000, **113**, 9901.

26 R. Lasser and K. Bickmann, Phase diagram of the Nb-T system, *J. Nucl. Mater.*, 1985, **132**, 24–28.

27 T. Schober and H. Wenzl, The systems NbH(D), Tall(D), VH(D):structures, phase diagrams, morphologies, methods of preparation. Hydrogen in metals II, *Top. Appl. Phys.*, 1978, **29**, 11–71.

28 F. M. Mazzolai and H. K. Birnbaum, Elastic constants and ultrasonic attenuation of the a-a′ phase of the Nb-H(D) system. I: results, *J. Phys. F: Met. Phys.*, 1985, **15**, 507–523.

29 S. Q. Wang and H. Q. Ye, Ab initio elastic constants for the lonsdaleite phases of C, Si Ge, *J. Phys.: Condens. Matter*, 2003, **15**, 5307–5314; C. Wei, J. L. Fan and H. R. Gong, Structural, thermodynamic, and mechanical properties of bulk La and A-La_2O_3, *J. Alloys Compd.*, 2015, **618**, 615–622.

30 C. P. Liang and H. R. Gong, Fundamental mechanism of tetragonal transitions in titanium hydride, *Mater. Lett.*, 2014, **115**, 252–255.

31 Z. J. Wu, E. J. Zhao, H. P. Xiang, *et al.*, Crystal structures and elastic properties of superhard IrN_2 and IrN_3 from first principles, *Phys. Rev. B: Condens. Matter Mater. Phys.*, 2007, **76**, 054115.

32 F. D. Murnaghan, The compressibility of media under extreme pressures, *Proc. Natl. Acad. Sci. U. S. A.*, 1944, **30**, 244; Q. Q. Ren, J. L. Fan and H. R. Gong, Work function and cohesion properties of W-Fe interfaces, *Mater. Lett.*, 2015, **145**, 205–208.

33 A. Reuss, Berechnung der Fließgrenze von Mischkristallen auf Grund der Plastizitätsbedingung für Einkristalle, *Z. Angew. Math. Mech.*, 1929, **9**, 49–58.

34 W. Voigt, *Lehrbuch der Kristallphysik*, B. G. Teubner, Leipzig, 1910.

35 G. Henkelman and B. P. Uberuaga, A climbing image nudged elastic band method for finding saddle points and minimum energy paths, *J. Chem. Phys.*, 2000, **113**(22), 9901–9904.

36 Y. Wu, Z. M. Wang, P. F. Liu, T. Bo, C. Y. Hao, C. H. Hu, Z. X. Cheng, B. T. Wang and H. Y. Zhou, Understanding of transition metal (Ru, W) doping into Nb for improved thermodynamic stability and hydrogen permeability: density functional theory calculations, *Phys. Chem. Chem. Phys.*, 2019, DOI: 10.1039/c9cp02012h.

37 J. W. Wang, Y. H. He and H. R. Gong, Various properties of Pd_3Ag/TiAl membranes from density functional theory, *J. Membr. Sci.*, 2015, **475**, 406–413.

38 Y. L. Liu, Y. Zhang, G. N. Luo and G. H. Lu, Structure, stability and diffusion of hydrogen in tungsten: A first-principles study, *J. Nucl. Mater.*, 2009, **390/391**, 1032–1034.

39 Y. L. Liu, Y. Zhang, H. B. Zhou, G. H. Lu, F. Liu and G. N. Luo, Vacancy trapping mechanism for hydrogen bubble formation in metal, *Phys. Rev. B: Condens. Matter Mater. Phys.*, 2009, **79**, 172103.

40 C. Duan, Y. L. Liu, H. B. Zhou, Y. Zhang, S. Jin, G. N. Luo and G. H. Lu, First-principles study on dissolution and diffusion properties of hydrogen in molybdenum, *J. Nucl. Mater.*, 2010, **404**, 109–115.

